Transactions of the Materials Research Society of Japan 33[4] 1085-1088 (2008)

Conducting properties of $M_{0.25}Ce_{0.75}O_{1.875}$ (M=Dy, Gd) sintered specimen fabricated by the combined process of pulsed electric current sintering and fast sintering

Hirokazu Suga[1,4], Toshiyuki Mori[1], Fei Ye[1], Ding Rong Ou[1], Toshiyuki Nishimura[2], John Drennan[3] and Hidehiko Kobayashi[4]
[1]Fuel Cell Materials Center, National Institute for Materials Science
1-1 Namiki, Tsukuba, Ibaraki, Japan
E-mail: MORI.Toshiyuki@nims.go.jp
[2]Nano Ceramics Center, National Institute for Materials Science
1-1 Namiki, Tsukuba, Ibaraki, Japan
[3]Centre for Microscopy and Microanalysis, The University of Queensland
St.Lucia, Brisbane, Queensland, 4072, Australia
[4]Graduate School of Science and Engineering, Saitama University
255 Shimo-okubo, Sakura-ku, Saitama city, Saitama, Japan

Dense $M_{0.25}Ce_{0.75}O_{1.875}$ (M=Dy, Gd) sintered specimens with different standard deviation of grain size distribution were fabricated using conventional sintering (CS), fast sintering (FS), pulsed electric current sintering (PECS) and a combined process of PECS and FS. To maximize the ionic conductivity in those doped ceria, we examined the relationship between the conducting properties and standard deviation values. A big standard deviation value (S.D. = 392 nm) was observed from $Dy_{0.25}Ce_{0.75}O_{1.875}$ CS specimen sintered at 1450°C for 6h (heating rate : 5°C/min). It was hard to observe the oxide ionic conducting phenomenon in that specimen at 500°C into the wide range of oxygen partial pressure (i.e. P_{O2}: 10^{-21} to 1 atm). On the other hand, the standard deviation observed from $Dy_{0.25}Ce_{0.75}O_{1.875}$ (PECS+FS) specimen was quite small (S.D. = 68 nm). The oxide conducting phenomenon was clearly observed into the (PECS+FS) specimen in the same measurement condition of conducting property. The similar result was obtained using $Gd_{0.25}Ce_{0.75}O_{1.875}$ specimens. This indicates that the control of in-homogeneity of microstructure is a key for an improvement of the oxide ionic conductivity in the doped CeO_2 sintered specimens.

Key words: Doped ceria, In-homogeneity of microstructure, Pulsed electric current sintering, Conducting properties, Oxygen partial pressure dependence of conductivity

1. INTRODUCTION

Tri-valent rare earth cation doped CeO_2 has been developed as a candidate for solid electrolyte in solid oxide fuel cells (SOFCs) operated at 'intermediate temperature (300-500 ° C)'. [1] The oxide ionic conductivity of doped CeO_2 is higher than that of yittria-stabilized ZrO_2 at the same temperature. Doped CeO_2, however, is easily reduced at anodic condition (oxygen partial pressure (P_{O2}): 10^{-21} atm). The electronic conductivity is developed by the reduction of CeO_2. The electronic conductivity in the doped CeO_2 makes open circuit voltage of fuel cells quite low. To develop doped CeO_2 compounds as electrolyte in SOFCs, the improvement of ionic conductivity of doped CeO_2 at both anode and cathode conditions is required.

In our previous work, [2] we examined the relationship between oxide ionic conductivity and microstructure in atomic scale of doped CeO_2 sintered specimens. Our nano-analysis tells us that the dopant cation is agglomerated in the micro-domain into the grain. It was concluded that oxide ionic conductivity of doped CeO_2 was lowed by the agglomeration of dopant cation in the sintered specimen. Also, the agglomeration level of dopant cation in Ho doped CeO_2 [3] which is semi-conductor was much higher than that in Y doped CeO_2 which is oxide ionic conductor. Those results clearly indicate that the in-homogeneity of microstructure should be improved to develop the oxide ionic conductivity of doped CeO_2 sintered specimens.

In the present work, the relationship between conducting properties and standard deviation of grain size distribution of doped CeO_2 was examined. To improve the in-homogeneity of microstructure, dense $M_{0.25}Ce_{0.75}O_{1.875}$ (M=Dy, Gd) sintered specimens with different standard deviation were fabricated using CS, FS, PECS and a combined process of PECS and FS. P_{O2} dependence of conductivity and activation energy recorded from sintered specimens were also investigated for conclusion about the relationship between conducting properties and in-homogeneity of microstructure of doped CeO_2.

2. EXPERIMENTAL

Nano-sized doped CeO_2 powders were prepared using ammonium carbonate co-precipitation method. The round-shaped nano sized precursor particles were prepared by aforementioned method. The precursor powders of Dy doped CeO_2 and Gd doped CeO_2 were calcined at 700 and 750 °C for 2h in oxygen gas flow, respectively. The average particle sizes of calcined powders were determined using FE-SEM. The dense $M_{0.25}Ce_{0.75}O_{1.875}$ (M=Dy, Gd) sintered specimens were fabricated using CS, FS, PECS, and (PECS + FS) methods. For CS process, calcined powders were molded under a pressure of 500kg/cm^2 and subjected to a rubber press at 2t/cm^2 (1t=10^{3}kg). Then the compact body was sintered at 1450-1550°C for 6h in air. The heating rate was 5°C/min. For FS process, the compact body of calcined powders was sintered at 1150 °C for 6h in Ar gas flow using dilatometer apparatus (TMA92, SETARAM). The heating rate was 80 °C/min. Figure 1 presents a schematic diagram of PECS apparatus (DR.SINTER SPS-1030, SPS Syntex).

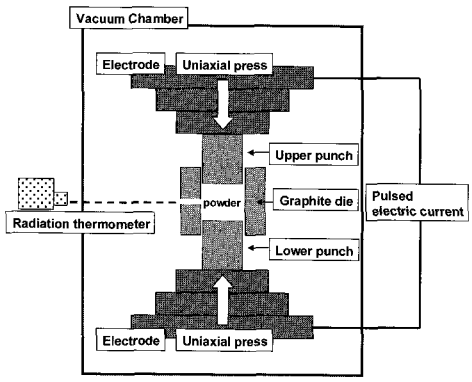

Figure 1 Schematic diagram of PECS apparatus.

For PECS process, approximately 2g of calcined powders were packed into graphite mold. The graphite sheets were inserted between calcined powders and graphite die. The graphite mold was placed at the center of electrode. And the electric current of 1000 A was applied under a pressure of 30 to 60 MPa. Sintering temperature ranged from 1050 to 1150 °C without holding time. Heating rate ranged from 10 to 1100 °C/min to change the applied electric power per unit pulse time (3.4ms) from 5 to 56 kJ/pulse. Since the applied electric power varied with the pattern of on/off ratio of applied pulse, the pattern of on/off ratio was changed from 1/9 – 12/2. In the combined process (PECS + FS), two step sintering process was performed. In the first step, the density of PECS specimens reached to approximately 80% of theoretical density. FS was performed at a temperature 25 ° C below PECS temperature. The sintering time of FS in a second step was 48 h. The heating rate was 100°C/min.

The microstructures of the sintered specimens were observed using field emission scanning electron microscope (FE-SEM, Hitachi S-5000). The average grain size and standard deviation (S.D.) of grain size distribution were calculated using image analysis software "Mac-View ver.4.0" by measuring approximately 300 grains. The average grain size was calculated as Heywood radius. And S.D. value was calculated by following equation;

$$S.D. = [\Sigma(D_i - D_{ave})^2 / n]^{1/2}$$

where D_{ave} is the average grain size, D_i is each grain size and n is a number of grains in the analysis area.

Bulk density of each sintered specimen was estimated using Archimedes method. Theoretical density of each composition was calculated using composition and lattice parameter. The lattice parameter was calculated using powder X-ray diffraction method. Correct lattice parameter was estimated by NaCl internal standard substance method. The relative density of each specimen was calculated using the ratio of the bulk density and theoretical density. For the electrical conductivity measurements, platinum electrodes were applied on both sides of sintered specimens at 1000°C. The conducting properties in the sintered specimens were measured by DC three-terminal measurements at 400° - 600°C. The oxygen partial pressure dependence of conductivity in the sintered specimens was measured at 500°C in oxygen, air, argon, wet hydrogen and dry hydrogen gas flow. A stable low P_{O2} atmosphere (i.e. P_{O2}: 10^{-15} atm) was made by zirconia oxygen pump under wet argon gas flow. And P_{O2} was determined by zirconia oxygen sensor.

3. RESULTS AND DISCUSSION

3.1 Densification behavior vs. in-homogeneity of microstructure

Since the specimen and the graphite mold were directly heated by applied current in PECS process, we concluded that the bulk density of specimens increased with an increase of the applied electric power. Figure 2 shows the relationship between the relative density of PECS specimen and applied electric power in PECS process.

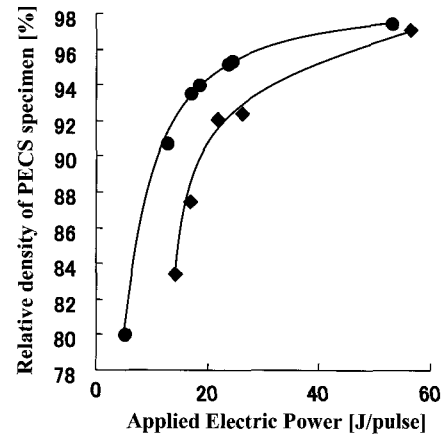

Figure 2 Relationship between relative densities of PECS specimens and applied electric power in PECS process. ◆ $Dy_{0.25}Ce_{0.75}O_{1.875}$ ● $Gd_{0.25}Ce_{0.75}O_{1.875}$

The results of Fig.2 almost agreed with our idea about densification behavior in PECS process. The densities of $Dy_{0.25}Ce_{0.75}O_{1.875}$ and $Gd_{0.25}Ce_{0.75}O_{1.875}$ PECS specimens reached to 97 % of theoretical density when applied electric power was above 50 J/pulse. This indicates that high applied electric power homogeneously heated almost all grain boundaries of sintered specimens and promoted homogeneous grain growth in PECS process.

Figure 3 displays SEM images recorded from $Dy_{0.25}Ce_{0.75}O_{1.875}$ sintered specimens which were fabricated using CS, FS, PECS and (PECS + FS) process.

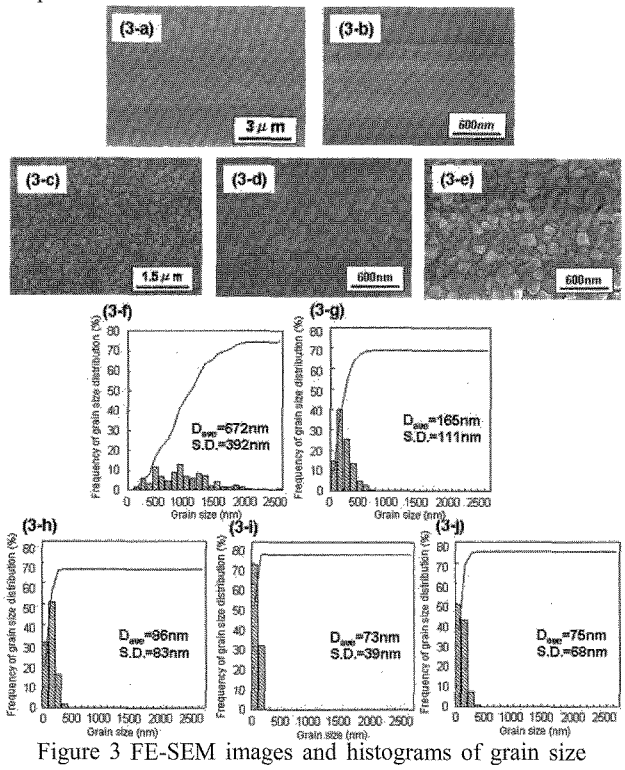

Figure 3 FE-SEM images and histograms of grain size distribution recorded from $Dy_{0.25}Ce_{0.75}O_{1.875}$ sintered specimens; CS specimen sintered at 1450°C-6h (5°C/min) ((3-a) and (3-f)), CS specimen sintered at 1150°C-6h (5°C/min) ((3-b) and (3-g)), FS specimen sintered at 1150°C-6h (80°C/min) ((3-c) and (3-h)), PECS specimen sintered at 1150°C-0min (900°C/min, on/off=1/9, 60MPa) ((3-d) and (3-i)), and PECS+FS specimen (1050°C-0min, 900°C/min + 1025°C-48h, 100°C/min) ((3-e) and (3-j)).

Also, the standard deviation value of grain size distribution recorded from each sintered specimen was shown in Fig.3. In the CS specimen sintered at 1450°C, a heterogeneous grain growth was observed. The grain size distribution and S.D. value recorded from aforementioned specimen was quite broad and big (S.D.= 392nm). And the grain size distribution recorded from CS specimen sintered at 1150°C becomes sharp, and its S.D. value was smaller than that of CS specimen sintered at 1450°C. But heterogeneous grain growth in the CS specimen sintered at lower temperature was still observed in Fig.3. On the other hand, the homogeneous grain growth in the FS specimen, (PECS+FS) specimen and PECS specimen was observed as shown in Fig.3. The highest homogeneity of microstructure was observed in PECS and (PECS + FS) specimens. The S.D. value recorded from PECS and (PECS + FS) specimens were 39nm and 68nm, respectively. Those values were much smaller than that of CS specimens. This indicates that in-homogeneity of microstructure can be minimized by the optimization of sintering conditions.

The relationship between sintering conditions and in-homogeneity of microstructure observed from $Gd_{0.25}Ce_{0.75}O_{1.875}$ specimens was almost same as $Dy_{0.25}Ce_{0.75}O_{1.875}$ series. Therefore, we conclude that in-homogeneity of micro-structure of doped CeO_2 is controllable by the optimization of sintering process if easy sinterable doped CeO_2 powders could be prepared as well as our case.

3.2 Conducting properties vs. in-homogeneity of microstructure

In the operation condition of SOFC, the electrolyte is in both of anode and cathode conditions. As consequence, the electrolyte has to keep high oxide ionic conductivity in wide range of P_{O2} (from 10^{-20} to 1 atm). To specify the influence of in-homogeneity of microstructure on conducting properties, the P_{O2} dependence of conductivity of $Dy_{0.25}Ce_{0.75}O_{1.875}$ sintered specimens at 500°C was examined as shown in Fig. 4.

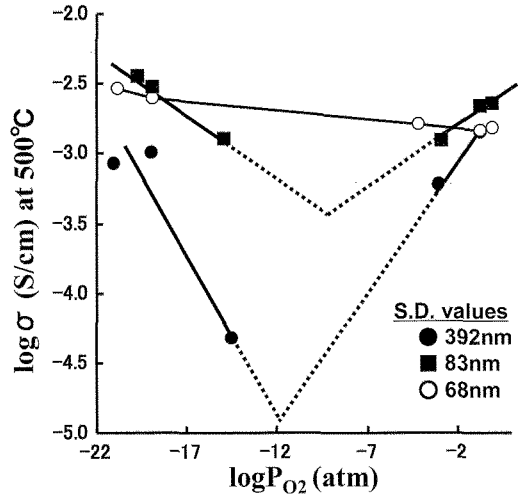

Figure 4 P_{O2} dependence of conductivity at 500°C recorded from $Dy_{0.25}Ce_{0.75}O_{1.875}$ sintered specimens; ●: CS specimen shown in Fig. 3-a, ■: FS specimen shown in Fig. 3-c and ○: (PECS+FS) specimen shown in Fig. 3-j.

As shown in Fig.4, it was hard to observe oxide ionic conducting phenomenon in the CS specimen with heterogeneous microstructure (● plot in Fig.4, S.D.: 392 nm) in the wide range of P_{O2}. This implies that the oxygen vacancies in the CS specimen with quite heterogeneous microstructure don't contribute to enhancement of oxide ionic conducting property in this specimen. In the micro-structure of aforementioned CS specimen, the degree of oxygen vacancy ordering would be in a quite high level, and the oxide ion could not be diffused through such heterogeneous microstructure. Since the heterogeneity of micro-structure can be improved by the optimization of sintering conditions, we examined the P_{O2} dependence of conductivity of FS specimen and (PECS + FS) specimen as demonstrated in Fig.4. The semi-conducting property observed from FS specimen became small as compared with CS specimen, even though chemical composition of FS specimen was exactly equal to that of CS specimen in Fig.4. This re-indicates that a control of in-homogeneity of microstructure makes oxide ionic conducting property a big improvement. This would be attributable to improvement of in-homogeneity in nano-scale of grain

interior and grain boundary regions of Dy doped CeO_2 sintered specimen. In addition, we can see one more interesting result in this figure. The P_{O2} dependence of conductivity of (PECS + FS) specimen was almost constant in relation to measured P_{O2}. Based on the results in Fig.4, we concluded that oxide ionic conducting properties in doped CeO_2 was strongly influenced by the in-homogeneity of microstructure. To maximize the potential of doped CeO_2, it is concluded that we must carefully analyze the micro-structural features and control the nano-in-homogeneity of microstructure.

Figure 5 presents temperature dependence of conductivity of $Dy_{0.25}Ce_{0.75}O_{1.875}$ sintered specimens with different S.D. values.

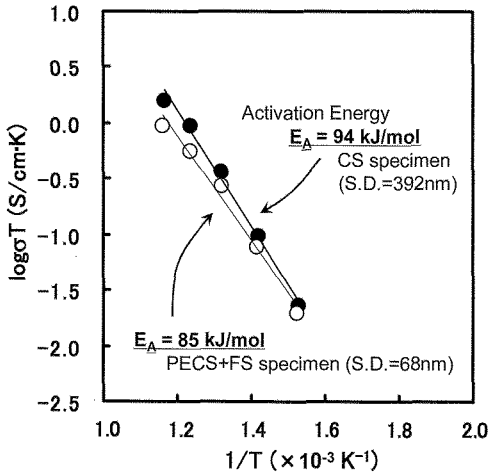

Figure 5 Arrhenius plots of conductivity recorded from $Dy_{0.25}Ce_{0.75}O_{1.875}$ CS specimen (S.D.=392nm, ●) and combined process (PECS + FS) specimen (S.D.=68nm, ○) in O_2 gas flow.

This Arrhenius plots also suggests that conducting mechanism between CS specimen with heterogeneous microstructure (S.D. : 392 nm) and (PECS + FS) specimen with homogeneous microstructure (S.D. : 68 nm) is quite different. The apparent activation energy measured from CS specimen (94kJ/mol) was much higher than that of (PECS + FS) specimen (85kJ/mol). The apparent activation energy measured from (PECS + FS) almost agreed with the previously reported activation energy of $Y_{0.25}Ce_{0.75}O_{1.875}$ sintered specimen which is oxide ionic conductor (83kJ/mol). [4] Since the previously reported activation energy in high temperature region (i.e. from 820°C to 1000°C) measured from Gd doped CeO_2 which clearly showed hole conductivity was 129kJ/mol, [5] we concluded that conducting mechanism of CS specimen with high S.D. value became close to the aforementioned doped CeO_2 which is semi-conductor. Taking all mentioned experimental results into account, it is concluded that the oxide ionic conductivity can be maximized in the Dy doped CeO_2 sintered bodies by the design of homogeneity in the doped CeO_2 specimens.

The relationship between standard deviation and ratio of σ_{max} / σ_{min} in the whole measured P_{O2} region is presented in Fig.6. In the case of oxide ionic conductor, the ratio of $\sigma_{max}/\sigma_{min}$ in the whole measured P_{O2} region would get close to 1.0 in Fig.6. It is because the P_{O2} dependence of oxide ionic conductivity becomes unity in the wide range of P_{O2}. Figure 6 suggests that the ratios of σ_{max} / σ_{min} recorded from Gd doped CeO_2 and Dy doped CeO_2 sintered specimens decreased with deceasing standard deviation of grain size distribution. When S.D. value was under 100nm, the slope of in-homogeneity of microstructure dependence of conducting property became steep. The ratio of $\sigma_{max}/\sigma_{min}$ got close to 1.0. This clearly suggests us that we have a chance to improve the oxide ionic conductivity of doped CeO_2 sintered bodies by a control of in-homogeneity of microstructure of the sintered specimens. Also we conclude that in-homogeneity at micro-meter scale is closely related to nano-in-homogeneity of microstructure. Since the semi-conducting property in doped CeO_2 is unusual in this measurement condition, further investigation of nano-in-homogeneity is needed to clarify the origin of the semi-conduction. We expect that quite high quality doped CeO_2 solid electrolytes will be designed by a control of nano-in-homogeneity of doped CeO_2 powders and sintered specimens.

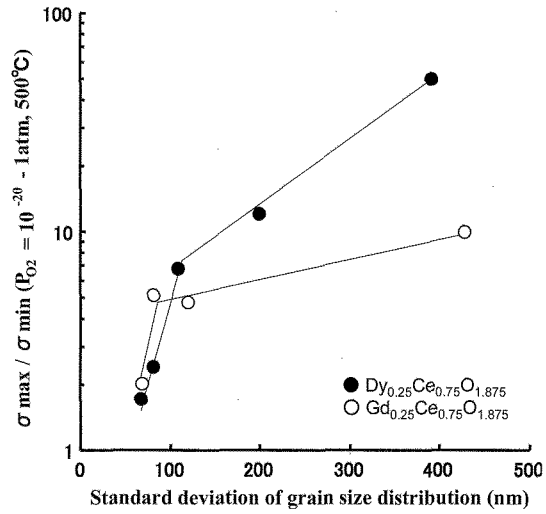

Figure 6 $\sigma_{max}/\sigma_{min}$ vs. S.D. value recorded from $M_{0.25}Ce_{0.75}O_{1.875}$ (M=Dy, Gd) sintered specimens.

4. SUMMARY

Dense $M_{0.25}Ce_{0.75}O_{1.875}$ (M=Dy, Gd) sintered specimens with different S.D. value (39 – 392 nm) were fabricated using CS, FS, PECS and (PECS+FS). Relationship between conducting properties and in-homogeneity of microstructures was examined to maximize the oxide ionic conductivity in the sintered specimen. It is concluded that the oxide ionic conductivity of doped CeO_2 is improved by a control of in-homogeneity of microstructure.

5. REFFERENCES

1. S.M.Haile, *Acta Materialia*, **51**, 5981-6000 (2003).
2. T.Mori, J.Drennan, J.H.Lee, J.G.Li and T.Ikegami, *Solid State Ionics*, **154-155**, 461-466 (2002).
3. D.R.Ou, T.Mori, F.Ye, J.Zou, G.Auchterlonie and J.Drennan, *J.Electrochem.Soc.*, **154**, B616-B622 (2007).
4. D.R.Ou, T.Mori, F.Ye, M.Takahashi, J,Zou and J.Drennan, *Acta Materialia*, **54**, 3737-3746 (2006).
5. F.M.Figueiredo, F.M.B.Marques and J.R.Frade, *J.Eur.Ceram.Soc.*, **19**, 807-810 (1999).

(Recieved December 9, 2007 ; Accepted September 1, 2008)